

Muon spin rotation studies of $\text{SmFeAsO}_{0.85}$ and $\text{NdFeAsO}_{0.85}$ superconductors

Rustem Khasanov,^{1,*} Hubertus Luetkens,¹ Alex Amato,¹ Hans-Henning Klauss,² Zhi-An Ren,³ Jie Yang,³ Wei Lu,³ and Zhong-Xian Zhao³

¹Laboratory for Muon Spin Spectroscopy, Paul Scherrer Institut, CH-5232 Villigen PSI, Switzerland

²IFP, TU Dresden, D-01069 Dresden, Germany

³National Laboratory for Superconductivity, Institute of Physics and Beijing National Laboratory for Condensed Matter Physics, Chinese Academy of Sciences, P.O. Box 603, Beijing 100190, People's Republic of China

(Received 13 August 2008; published 29 September 2008)

Measurements of the in-plane magnetic-field penetration depth λ_{ab} in Fe-based superconductors with the nominal composition $\text{SmFeAsO}_{0.85}$ ($T_c \approx 52$ K) and $\text{NdFeAsO}_{0.85}$ ($T_c \approx 51$ K) were carried out by means of muon-spin rotation. The absolute values of λ_{ab} at $T=0$ were found to be 189(5) and 195(5) nm for Sm and Nd substituted samples, respectively. The analysis of the magnetic penetration depth data within the Uemura classification scheme, which considers the correlation between the superconducting transition temperature T_c and the effective Fermi temperature T_F , reveals that both families of Fe-based superconductors (with and without fluorine) fall to the same class of unconventional superconductors.

DOI: 10.1103/PhysRevB.78.092506

PACS number(s): 74.70.-b, 76.75.+i

The recent discovery of the Fe-based layered superconductor $\text{LaO}_{1-x}\text{F}_x\text{FeAs}$ (Ref. 1) with the transition temperature $T_c=26$ K has triggered an intense research in the oxypnictides. In its wake, a series of superconductors with T_c onset of up to 55 K have been synthesized successively by substituting La with other rare-earth (Re) ions such as Sm, Ce, Nd, Pr, and Gd.^{2,3} Recently the family of the oxypnictide superconductors ReFeAsO_{1-x} with the doping induced by oxygen vacancies instead of fluorine substitution were synthesized.^{4,5}

One of the questions, which awaits to be explored, is to which class of the superconducting materials the discovered Fe-based superconductors belong. The search for relations between the various physical variables such as transition temperature, magnetic-field penetration depth, electrical conductivity, energy gap, Fermi temperature, etc. may help to answer this question. Among others, there is a correlation between T_c and the zero-temperature inverse squared magnetic-field penetration depth [$\lambda^{-2}(0)$] that generally relates to the zero-temperature superfluid density (ρ_s) in terms of $\rho_s \propto \lambda^{-2}(0)$. In various families of underdoped high-temperature cuprate superconductors (HTSs), there is the empirical relation $T_c \propto \rho_s \propto \lambda^{-2}(0)$, first identified by Uemura and co-workers.^{6,7} In this respect it is rather remarkable that the magnetic-field penetration measurements on $\text{LaO}_{1-x}\text{F}_x\text{FeAs}$ ($x=0.1$ and 0.075) (Ref. 8) and $\text{SmO}_{0.82}\text{F}_{0.18}\text{FeAs}$ (Ref. 9) result in values of the superfluid density, which are close to the Uemura line for hole doped cuprates, indicating that the superfluid is also very dilute in the oxypnictides.

In this Brief Reports we focus on the different classification scheme proposed by Uemura and co-workers,^{7,10} which considers the correlation between T_c and the effective Fermi temperature T_F determined from measurements of the in-plane magnetic penetration depth λ_{ab} . Within this scheme strongly correlated unconventional superconductors, such as HTSs, heavy fermions, Chevrel phases, or organic superconductors, form a common but distinct group, characterized by a universal scaling of T_c with T_F such that $1/10 > T_c/T_F > 1/100$. We show that within the Uemura classification scheme both families of oxypnictide superconductors (with

and without fluorine) fall to the same class of unconventional superconductors.

Details on the sample preparation for $\text{SmFeAsO}_{0.85}$ ($T_c \approx 52$ K) and $\text{NdFeAsO}_{0.85}$ ($T_c \approx 51$ K) can be found elsewhere.⁵ Both samples studied in the present work were in the form of sintered powders. Zero-field (ZF), longitudinal-field (LF), and transverse-field (TF) muon-spin rotation (μSR) experiments were performed at the πM3 beam line at the Paul Scherrer Institute (Villigen, Switzerland). Here LF and TF denote the cases when the magnetic field is applied parallel (LF) and perpendicular (TF) to the initial muon-spin polarization. ZF and LF μSR measurements are used to probe the intrinsic magnetic properties of a sample. While ZF μSR provides information on the internal magnetic-field distribution, the complementary application of LF measurements allows discrimination between static and fluctuating fields. In TF μSR measurements, the additional relaxation due to the inhomogeneous internal field distribution in the vortex phase of the type-II superconductors allows to extract, e.g., the absolute value of the magnetic penetration depth. For detailed description of ZF, LF, and TF μSR techniques, see Ref. 11. During the experiments we were mostly concentrated on $\text{SmFeAsO}_{0.85}$, which shows the highest T_c among other oxypnictide superconductors discovered until now. For $\text{NdFeAsO}_{0.85}$ we studied only the temperature dependence of the superfluid density in a field of 0.2 T.

First we present the results of ZF and LF μSR experiments on $\text{SmFeAsO}_{0.85}$. The recent ZF μSR studies of the parent LaOFeAs compound reveal that there are two interstitial lattice sites where muons come to the rest, namely, close to the Fe magnetic moments within the FeAs layers and near the LaO planes.¹² Therefore, the ZF and the LF muon-time spectra for $T \leq 80$ K were analyzed by using the following depolarization function:

$$P^{\text{ZF,LF}}(t) = A_{\text{slow}} \exp(-\Lambda_{\text{slow}} t) + A_{\text{fast}} \exp(-\Lambda_{\text{fast}} t). \quad (1)$$

Here A_{slow} (A_{fast}) and Λ_{slow} (Λ_{fast}) are the asymmetry and the depolarization rate of the slow (fast) relaxing component, respectively. The whole set of ZF (LF) data was fitted simul-

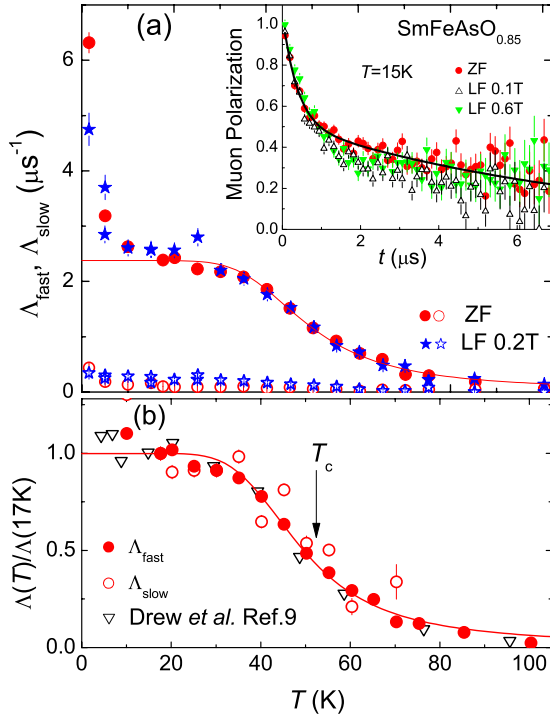


FIG. 1. (Color online) (a) Temperature dependences of the fast (Λ_{fast}) and the slow (Λ_{slow}) components of the ZF and the LF muon depolarization rates of $\text{SmFeAsO}_{0.85}$. (b) $\Lambda_{\text{fast}}(T)$ and $\Lambda_{\text{slow}}(T)$ normalized to their values at $T=17$ K. Open triangles represents the normalized data of $\text{SmO}_{0.82}\text{F}_{0.18}\text{FeAs}$ from Ref. 9. The inset in (a) shows the ZF and the LF μSR time spectra of $\text{SmFeAsO}_{0.85}$ measured at $T=15$ K. The solid lines in (a) and (b) are the fits of Eq. (2) to ZF $\Lambda_{\text{fast}}(T)$.

taneously with the ratio $\Lambda_{\text{slow}}/\Lambda_{\text{fast}}$ as a common parameter and the relaxations (Λ_{slow} and Λ_{fast}) as individual parameters for each particular data point. The total asymmetry $\Lambda_{\text{slow}} + \Lambda_{\text{fast}}$ was kept constant within each set of the data (ZF or LF). Above 80 K the fit is statistically compatible with a single exponential component only. The results of the analysis and the representative ZF and LF muon-time spectra are shown in Fig. 1.

From the data presented in Fig. 1 the following important points emerge: (i) Both $\Lambda_{\text{fast}}(T)$ and $\Lambda_{\text{slow}}(T)$ measured in the zero and the longitudinal (up to 0.6 T) fields coincide within almost the whole temperature region. This, together with the exponential character of the muon polarization decay, reveals the existence of fast electronic fluctuations measurable within the μSR time window. Since no sign of static or dynamic magnetism has been observed in optimally doped $\text{LaO}_{0.9}\text{F}_{0.1}\text{FeAs}$,⁸ we attribute the observed relaxation to be due to fluctuations of the Sm magnetic moments. Assuming the fluctuation rate with a temperature dependence $\nu \sim \exp(E_0/k_B T)$ (E_0 is the activation energy) and accounting for the saturation of $\Lambda \approx \Lambda_0$ at $10 \text{ K} \lesssim T \lesssim 35 \text{ K}$, the relaxation is expected to follow:¹³

$$\frac{1}{\Lambda} = \frac{1}{\Lambda_0} + \frac{1}{C \exp(E_0/k_B T)}. \quad (2)$$

The fit of Eq. (2) to the experimental ZF Λ_{fast} data yields $\Lambda_{0,\text{fast}} = 2.38(6) \mu\text{s}^{-1}$, $C = 0.012(2) \mu\text{s}$, and $E_0 = 23(2) \text{ meV}$.

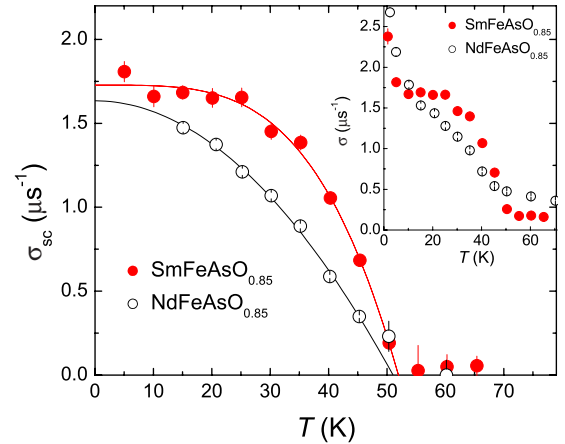


FIG. 2. (Color online) Temperature dependences of $\sigma_{\text{sc}} \propto \lambda_{\text{ab}}^{-2}$ for $\text{SmFeAsO}_{0.85}$ and $\text{NdFeAsO}_{0.85}$ measured after field cooling the samples in $\mu_0 H = 0.2$ T. The inset shows the Gaussian depolarization rate σ .

This kind of activated process can be anticipated for a thermal population of Sm crystal-field levels. (ii) The fact that both the slow and the fast relaxation rates exhibit similar temperature dependences [see Fig. 1(b)] strongly suggests that there is a common source for both relaxations. The magnitudes of Λ_{fast} and Λ_{slow} are thus related to the different couplings between muons and Sm moments at the distinct muon stopping sites. (iii) There are no features appearing in the vicinity of the superconducting transition. Figure 1(b) implies that Λ_{fast} increases continuously with decreasing temperature. This may suggest that the magnetic fluctuations responsible for the effects seen in Fig. 1 are not related to superconductivity. It is worth mentioning that, in systems exhibiting an interplay between the superconductivity and magnetism, the slowing down of the spin fluctuations (increase in Λ) correlates with T_c (see, e.g., Ref. 14). Another argument comes from the comparison of $\Lambda_{\text{fast}}(T)$ for $\text{SmFeAsO}_{0.85}$ ($T_c \approx 52$ K), studied here, with that reported by Drew *et al.*⁹ for $\text{SmO}_{0.82}\text{F}_{0.18}\text{FeAs}$ ($T_c \approx 45$ K) [see Fig. 1(b)]. Apparently the Sm spin fluctuations are independent of T_c . (iv) The fast increase in both Λ_{fast} and Λ_{slow} below 5 K is most probably associated with additional local-field broadening due to the ordering of the Sm moments.^{9,15}

The superconducting properties of $\text{SmFeAsO}_{0.85}$ and $\text{NdFeAsO}_{0.85}$ were studied in the TF μSR experiments. The temperature scans were made after cooling the samples from above T_c down to 1.7 K in $\mu_0 H = 0.2$ T. Following Hayano *et al.*¹⁶ it can be shown that the effect of fast fluctuations on the longitudinal and transverse depolarizations becomes similar. By taking this into account the TF μSR data were analyzed by using the following functional form:

$$P^{\text{TF}}(t) = P^{\text{LF}}(t) \exp(-\sigma^2 t^2/2) \cos(\gamma_\mu B t + \phi). \quad (3)$$

Here B is the average field inside the sample, $\gamma_\mu = 2\pi \times 135.5342 \text{ MHz/T}$ is the muon gyromagnetic ratio, ϕ is the initial phase, σ is the Gaussian relaxation rate, and $P^{\text{LF}}(t)$ is described by Eq. (1). σ vs T dependences for $\text{SmFeAsO}_{0.85}$ and $\text{NdFeAsO}_{0.85}$ are shown in the inset of Fig. 2. As it states

in Ref. 17 the Gaussian relaxation rate σ for a highly anisotropic type-II superconductor obeying, in addition, low-temperature magnetic ordering consists of a superconducting ($\sigma_{sc} \propto \lambda_{ab}^{-2}$), a magnetic (σ_m), and a small nuclear magnetic-dipole (σ_{nm}) contribution. We may conclude that, therefore, a continuous increase in σ below T_c relates to appearance of superconductivity while the sharp rise of σ at low temperatures is due to extra Sm (Refs. 9 and 15) and Nd (Ref. 18) orderings [see inset of Fig. 2 and ZF $\Lambda_{fast}(T)$ data in Fig. 1(a)]. Because σ_m is only present at low temperatures, data points below 5 K for SmFeAsO_{0.85} and 10 K for NdFeAsO_{0.85} were excluded in the analysis. The superconducting contribution ($\sigma_{sc} \propto \lambda_{ab}^{-2}$) was then determined by subtracting in quadrature σ_{nm} measured above T_c from σ and is presented in the main panel of Fig. 2.

The data in Fig. 2 were fitted with the power law $\sigma_{sc}(T)/\sigma_{sc}(0) = 1 - (T/T_c)^n$ with $\sigma_{sc}(0)$, n , and T_c as free parameters. The fit yields $\sigma_{sc}(0) = 1.73(5) \mu\text{s}^{-1}$, $T_c = 52.0(2)$ K, and $n = 3.74(16)$, and $\sigma_{sc}(0) = 1.63(5) \mu\text{s}^{-1}$, $T_c = 51.0(3)$ K, and $n = 1.98(14)$ for SmFeAsO_{0.85} and NdFeAsO_{0.85}, respectively. At the present stage we are not going to discuss the temperature dependences of σ_{sc} . We would only mention that the power-law exponent $n = 3.74(16)$ is close to the universal two-fluid value $n = 4$ while $n = 1.98(14)$ is close to $n = 2$, observed in a case of dirty d -wave superconductors.

As is shown by Brandt,¹⁹ σ_{sc} for anisotropic powder superconductor may be directly related to the in-plane magnetic penetration depth λ_{ab} via

$$\frac{\sigma_{sc}^2}{\gamma_\mu^2} = 0.00371 \frac{\Phi_0^2}{\lambda_{eff}^4} = 0.00126 \frac{\Phi_0^2}{\lambda_{ab}^4}, \quad (4)$$

where $\Phi_0 = 2.068 \times 10^{-15}$ Wb is the magnetic-flux quantum. Here we also take into account that in anisotropic superconductors, such as Fe-based oxypnictides,²⁰ the effective magnetic penetration depth λ_{eff} , measured in μSR experiments, is solely determined by the in-plane penetration depth as $\lambda_{eff} = 1.31\lambda_{ab}$.²¹ From measured $\sigma_{sc}(0)$'s the absolute values of the in-plane magnetic penetration were found to be $\lambda_{ab}(0) = 189(5)$ nm for SmFeAsO_{0.85} and $\lambda_{ab}(0) = 195(5)$ nm for NdFeAsO_{0.85}.

The magnetic-field dependence of ($\sigma_{sc} \propto \lambda_{ab}^{-2}$) for SmFeAsO_{0.85} measured at $T = 15$ K is shown in Fig. 3. At low fields a maximum in $\sigma_{sc}(H)$ is observed followed by a decrease in the relaxation rate up to the highest fields. Consideration of the ideal triangular vortex lattice of an isotropic s -wave superconductor within the Ginsburg-Landau approach leads to the following expression for the magnetic-field dependence of the second moment of the magnetic-field distribution:²²

$$\sigma_{sc}[\mu\text{s}^{-1}] = 4.83 \times 10^4 (1 - B/B_{c2}) \times [1 + 1.21(1 - \sqrt{B/B_{c2}})^3] \lambda^{-2}[\text{nm}]. \quad (5)$$

Here B is the magnetic induction, which for applied field in the region $H_{c1} \ll H \ll H_{c2}$ is $B \approx \mu_0 H$ (H_{c1} is the first critical field, and $B_{c2} = \mu_0 H_{c2}$ is the upper critical field). According to Ref. 22, Eq. (5) describes with less than 5% error the field variation of σ_{sc} for an ideal triangular vortex lattice and

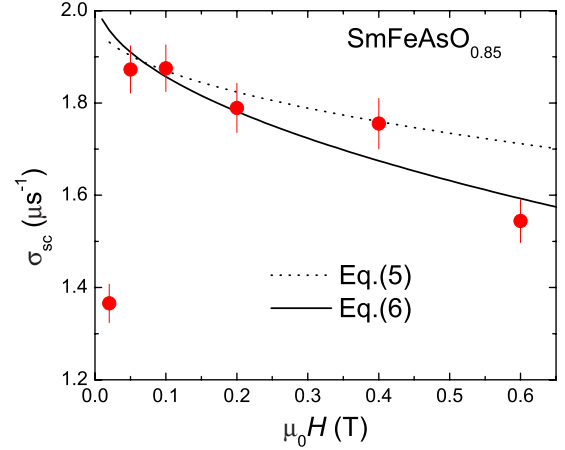


FIG. 3. (Color online) ($\sigma_{sc} \propto \lambda_{ab}^{-2}$) as a function of applied field H for SmFeAsO_{0.85}. Each point was obtained after field cooling the sample from above T_c to $T = 15$ K in the corresponding magnetic field. The solid and the dashed lines represent the results of analysis by means of Eqs. (5) and (6).

holds for type-II superconductors with the value of the Ginzburg-Landau parameter $\kappa \geq 5$ in the range of fields $0.25/\kappa^{1.3} \leq B/B_{c2} \leq 1$. Since we are not aware of any reported values of the second critical field for SmFeAsO_{0.85}, we used $B_{c2}(15 \text{ K}) \approx 80$ T obtained from $B_{c2}(0) \approx 100$ T reported by Senatore *et al.*²³ for SmO_{0.85}F_{0.15}FeAs. The black dotted line, derived by using Eq. (5), corresponds to $\lambda_{ab} = 232$ nm. Figure 3 implies that the experimental $\sigma_{sc}(H)$ depends stronger on the magnetic field than it is expected in a case of fully gaped s -wave superconductor. We have two possible explanations. (i) As shown by Amin *et al.*²⁴ the field dependent correction to ρ_s may arise from the nonlocal and nonlinear responses of a superconductor with nodes in the energy gap to the applied magnetic field. The solid line represents the result of the fit by means of the relation:

$$\frac{\rho_s(H)}{\rho_s(H=0)} = \frac{\sigma_{sc}(H)}{\sigma_{sc}(H=0)} = 1 - K \cdot \sqrt{H}, \quad (6)$$

which takes into account the nonlinear correction to ρ_s for a superconductor with a d -wave energy gap.²⁵ Here the parameter K depends on the strength of nonlinear effect. Since Eq. (6) is valid for the intermediate fields ($H_{c1} \ll H \ll H_{c2}$), only the points above 0.02 T were considered in the analysis. (ii) Strong dependence of σ_{sc} on magnetic field is observed in two-gap superconductors such as MgB₂ (Ref. 26) and NbSe₂,²⁷ and is explained by the faster suppression of the contribution of the smaller gap to the total superfluid density with increasing field.

Now we focus on the Uemura classification scheme, which considers the correlation between the superconducting transition temperature T_c and the effective Fermi temperature T_F determined from measurements of the penetration depth. Using this parametrization, Uemura *et al.*⁷ confirmed a close correlation between T_c and T_F . HTSs, heavy fermion, organic, fullerene, and Chevrel phase superconductors all follow a similar linear trend with $1/100 < T_c/T_F < 1/10$, in contrast to the conventional BCS superconductors (Nb, Sn, Al,

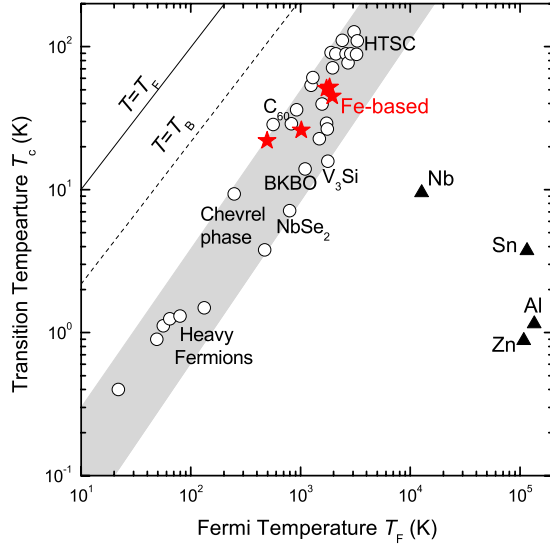


FIG. 4. (Color online) The superconducting transition temperature T_c vs the effective Fermi temperature T_F . The unconventional superconductors fall within a common band for which $1/100 < T_c/T_F < 1/10$, as indicated by the gray region in the figure. The dashed line corresponds to the Bose-Einstein condensation temperature T_B (see Ref. 7 for details). The points for $\text{SmFeAsO}_{0.85}$ and $\text{NdFeAsO}_{0.85}$ calculated from $\lambda_{ab}(0)$ values obtained in the present study and that for $\text{LaO}_{1-x}\text{F}_x\text{FeAs}$ ($x=0.1, 0.075$) (Ref. 8) and $\text{SmO}_{0.82}\text{F}_{0.18}\text{FeAs}$ (Ref. 9) are shown by solid red stars.

etc) for which $T_c/T_F < 1/1000$. The ‘‘Uemura plot’’ of $\log(T_c)$ vs $\log(T_F)$, shown in Fig. 4, thus appears to discriminate between the ‘‘unconventional’’ and ‘‘conventional’’ superconductors. The T_B represents the Bose-Einstein condensation temperature for a noninteracting three-dimensional Bose gas having the boson density $n_B = n_s/2$ and mass $m_B = 2m^*$. Intriguingly, all the unconventional superconductors

are found to have values of T_c/T_B in the range of $1/3$ – $1/30$, thereby emphasizing the proximity of these systems to Bose-Einstein-like condensation.

Following suggestions of Uemura *et al.*,⁷ the effective Fermi temperatures of the Fe-based superconductors were calculated as

$$k_B T_F = \hbar \pi c_{\text{int}} \frac{n_s}{m_{ab}^*} \propto c_{\text{int}} \sigma_{sc}. \quad (7)$$

Here $n_s/m_{ab}^* = \rho_s$ is the in-plane superfluid density, which within the London approach is proportional to λ_{ab}^{-2} and, thus, to σ_{sc} ($n_s/m_{ab}^* \propto \lambda_{ab}^{-2} \propto \sigma_{sc}$), n_s is the charge-carrier concentration, m_{ab}^* is the in-plane charge-carrier mass, and c_{int} is the distance between the conducting planes. The points for $\text{SmFeAsO}_{0.85}$ and $\text{NdFeAsO}_{0.85}$, and that obtained from $\lambda_{ab}(0)$ values of $\text{LaO}_{1-x}\text{F}_x\text{FeAs}$ ($x=0.1$ and 0.075) (Ref. 8) and $\text{SmO}_{0.82}\text{F}_{0.18}\text{FeAs}$ (Ref. 9) are shown in Fig. 4 by solid red stars. As is seen the Fe-based superconductors follow the same linear trend as is established for various unconventional materials, suggesting that they all probably share the common condensation mechanism.

To conclude, measurements of the in-plane magnetic-field penetration depth λ_{ab} in superconductors $\text{SmFeAsO}_{0.85}$ ($T_c \simeq 52$ K) and $\text{NdFeAsO}_{0.85}$ ($T_c \simeq 51$ K) were carried out by means of muon-spin rotation. The absolute values of λ_{ab} at $T=0$ were estimated to be $189(5)$ and $195(5)$ nm for Sm and Nd substituted samples, respectively. The analysis within the Uemura classification scheme, considering the correlation between the superconducting transition temperature T_c and the effective Fermi temperature T_F , reveal that both families of Fe-based superconductors (with and without fluorine) fall to the same class of unconventional superconductors.

This work was performed at the Swiss Muon Source ($S\mu S$), Paul Scherrer Institute (PSI, Switzerland).

*rustem.khasanov@psi.ch

¹Y. Kamihara *et al.*, *J. Am. Chem. Soc.* **130**, 3296 (2008).
²Z.-A. Ren *et al.*, *Chin. Phys. Lett.* **25**, 2215 (2008).
³Z.-A. Ren *et al.*, *Mater. Res. Innovations* **12**, 1 (2008).
⁴J. Yang *et al.*, *Supercond. Sci. Technol.* **21**, 082001 (2008).
⁵Z.-A. Ren *et al.*, *Europhys. Lett.* **83**, 17002 (2008).
⁶Y. J. Uemura *et al.*, *Phys. Rev. Lett.* **62**, 2317 (1989).
⁷Y. J. Uemura *et al.*, *Phys. Rev. Lett.* **66**, 2665 (1991).
⁸H. Luetkens *et al.*, *Phys. Rev. Lett.* **101**, 097009 (2008).
⁹A. J. Drew *et al.*, *Phys. Rev. Lett.* **101**, 097010 (2008).
¹⁰A. D. Hillier *et al.*, *Appl. Magn. Reson.* **13**, 95 (1997).
¹¹A. Amato, *Rev. Mod. Phys.* **69**, 1119 (1997).
¹²H. H. Klauss *et al.*, *Phys. Rev. Lett.* **101**, 077005 (2008).
¹³T. Lancaster *et al.*, *J. Phys.: Condens. Matter* **16**, S4563 (2004).
¹⁴A. Amato *et al.*, *Physica B (Amsterdam)* **326**, 369 (2003).

¹⁵L. Ding *et al.*, *Phys. Rev. B* **77**, 180510(R) (2008).

¹⁶R. S. Hayano *et al.*, *Phys. Rev. B* **20**, 850 (1979).

¹⁷R. Khasanov *et al.*, *Phys. Rev. B* **76**, 094505 (2007).

¹⁸Y. Qiu *et al.*, arXiv:0806.2195 (unpublished).

¹⁹E. H. Brandt, *Phys. Rev. B* **37**, 2349 (1988).

²⁰J. Jaroszynski *et al.*, *Phys. Rev. B* **78**, 064511 (2008); S.

Weyeneth *et al.*, arXiv:0806.1024 (unpublished).

²¹V. I. Fesenko *et al.*, *Physica C* **176**, 551 (1991).

²²E. H. Brandt, *Phys. Rev. B* **68**, 054506 (2003).

²³C. Senatore *et al.*, *Phys. Rev. B* **78**, 054514 (2008).

²⁴M. H. S. Amin *et al.*, *Phys. Rev. Lett.* **84**, 5864 (2000).

²⁵I. Vekhter *et al.*, *Phys. Rev. B* **59**, 1417 (1999).

²⁶S. Serventi *et al.*, *Phys. Rev. Lett.* **93**, 217003 (2004).

²⁷J. Sonier *et al.*, *Rev. Mod. Phys.* **72**, 769 (2000).